Histol Histopathol (2007) 22: 389-397

http://www.hh.um.es

Histology and Histopathology

Cellular and Molecular Biology

Microencephaly and microphthalmia in rat fetuses by busulfan

S. Furukawa, K. Usuda, M. Abe and I. Ogawa

Biological Research Laboratories, Nissan Chemical Industries, Ltd, Japan

Summary. Microencephaly and microphthalmia in the embryos/fetuses from rats exposed to busulfan were histopathologically examined. Busulfan was intraperitoneally administered at 10 mg/kg on gestation days (Days) 12, 13 and 14, and then embryos/fetuses were harvested on Days 14.5, 15, 16 and 21. In the treated group on Day 21, all fetuses were small with reduced body weight, with microencephaly and microphthalmia. On Days 14.5, 15 and 16, apoptotic cells were increased in the neuroepithelium and the neural retina with a width reduction and a decrease in cell density, and the lens epithelial cells histopathologically. Mitotic inhibition was observed in the neuroepithelium, neural retina and equatorial zone of the lens. On Day 21, the cerebral cortex and the retina became markedly thinner. The lens fibers showed swollen, fragmentary and vacuolar formation in the cranial portion accompanied with small lens sizes. The anti-proliferative effects of busulfan brings about a lack of cell populations required for the normal organogenesis of the brain and eye, and leads to microencephaly and microphthalmia, featuring hypoplasia of cerebrum and hypoplasia of retina and lens with cataract, respectively.

Key words: Busulfan, Fetus, Microencephaly, Microphthalmia, Rat

Introduction

Vulnerable periods during the development of the central nervous system are sensitive to environmental insults, as they are dependent on the temporal and spatial emergence of critical developmental processes, such as proliferation, migration, differentiation, synaptogenesis, myelination, and apoptosis (Rice and Barone, 2000). In normal neocortical development, the neuroepithelial cells in the dorsal layer of the neuroepithelium actively synthesize DNA. Postmitotic neurons migrate out of the neuroepithelium and form the preplate (O'Leary and Koester, 1993; Gressens, 2000). This process is highly sensitive to various physical effects, and chemical and biological agents. Neuronal migration disorders are major causes of microencephaly in experimental animals. Excessive neuron death is one of the most important mechanisms inducing neuronal migration disturbance in the developing cerebral cortex. On the other hand, anophthalmia or microphthalmia is caused by failure, suppression or degeneration during optic organogenesis (Szabo, 1989). Experimentally induced microencephaly and microphthalmia have been reported with many physical effects and chemical agents.

Busulfan, an alkylating agent, has been used as an anti-neoplastic agent for the treatment of chronic myeloid leukemia during pregnancy, and is a primary carcinogen and a clastogen (Bishop and Wasson, 1986). It is also known as a teratogen, inducing microencephaly and microphthalmia, and has ovarian and testicular toxicity with reduced the number of germ cells in rats (Nagai, 1972; Kasuga and Takahashi, 1986). In addition, busulfan induces anophthalmia, microtia, microrostellum, micrognathia, microabdomen, micromelia, oligodactylia, brachydactylia, vestigial tail, short tail, anasarca, etc. in rats and mice (Nagai, 1972). However, there are no reports that describe a detailed sequence of histopathological changes of the brain and eye in the fetuses following busulfan administration to dams in rats. In the present study, the brain and eye in the fetuses/embryos from rats exposed to busulfan during gestation days (Days) 12-14 were examined histopathologically in order to clarify the morphological changes of microencephaly and microphthalmia in the early developmental stage.

Offprint requests to: Satoshi Furukawa, Biological Research Laboratories, Nissan Chemical Industries, Ltd., 1470 Shiroaka, Minamisaitama Saitama 349-0294, Japan. e-mail: furukawa@nissanchem.co.jp

Materials and methods

Animals

A total of 32 pregnant specific pathogen-free Wistar Hannover GALAS rats (CLEA Japan, Inc., Japan), at approximately 10-14 weeks of age, were purchased. The animals were single-housed in wire-mesh cages in an air-conditioned room (22±2°C; humidity, 55±10%; light cycle, 12 hr/day). Feed (Oriental Yeast Co., LTD., Japan) and water were available *ad libitum*.

Experimental design

Day 0 was designated as the day when the presence of vaginal plug was identified. Busulfan (Wako Pure Chemical Industries, Japan) was suspended in olive oil and administered intraperitoneally (i.p) (0.5 ml/100 g body weight of rats). The pregnant rats were randomly allocated to 2 groups of 16 rats each. Animals were treated daily at dose levels of 0 (olive oil only) or 10 mg/kg during Days 12-14, early stage of cerebral cortex development and stage of lens and retina development (DeSesso, 2005). The dose level of 10 mg/kg i.p. was previously reported to induce a reduction in the number of oocytes at birth and sterilization in rats (Hirshfield, 1994). All treatments were made between 10 and 11 a.m. Four rats from each group were sampled on Days 14.5, 15, 16 and 21. Animals were weighed, euthanized by exsanguination under diethyl ether anesthesia, and necropsied. The embryos/fetuses were removed from the uterus, weighed, and examined for external malformation with the aid of a dissecting microscope. The placentas were also removed and weighed. The embryos/fetuses were fixed in 10% neutral buffered formalin. The brains of 6 fetuses from each dam in each group on Day 21 were weighed and the length of cerebrum and total brain were measured (Fig. 1). Length ratio of cerebrum was determined by dividing the sagittal length of cerebral hemisphere by the longitudinal length of total brain (cerebrum, midbrain and cerebellum). All experiments were conducted according to the Guideline for Animal Experimentation, Japanese Association for Laboratory Animal Science, 1987.

Histological examination

Four embryonic brains including eyes on Days 14.5, 15 and 16, and 6 fetal brains and 3 fetal eyes on Day 21 were selected randomly from each litter and trimmed coronally for histopathological evaluation in the way shown in Figure 1. In addition, 2 embryonic brains on Days 14.5, 15 and 16 were trimmed longitudinally. These tissues were embedded in paraffin, sectioned at a 4-μm thickness, and stained routinely with hematoxylin and eosin (H&E) for histopathological examination. In addition, the number of the mitosis (mitotic index) for the neuroepithelium in the telencephalon, neural retina, and lens was counted in the cerebral cortex and eyes of one side in four embryos trimmed coronally on Days 14.5, 15 and 16 by light microscopy with a x 40 objective from each litter. Immunohistochemical stainings, involving antibody to proliferating cell nuclear antigen (PCNA) (PCNA, PC10: DAKO, Japan) according to the avidin-biotin complex (ABC) method (VECTSTAIN ABC Kit: Vector Laboratories Inc., Canada) and *in situ* TdT-mediated dUTP nick end labeling (TUNEL) (ApopTag^{R}: Chemicon International, USA) were performed in these tissues. The nomenclature for the layers of developing brain used was in accordance to that used by O'Leary and Koester (1993), Ueno et al., (2002a) and Bayer and Altman (2004) (Fig. 1).

Electron microscopic examination

Small pieces of the telencephalic wall from one formalin-fixed treated embryo on Day 14.5 were postfixed in 1% solution of osmium tetroxide, dehydrated in ethanol and embedded in Epon 812. Ultrathin sections were stained with uranyl acetate and lead citrate.

Statistical analysis

Means and standard error (SE) of the individual litter values were calculated. Continuous data were analyzed with the F test. When variances were homogeneous, the Student t-test was performed. The Aspin-Welch *t*-test was performed when variances were not homogeneous. The level of significance was set at $p<0.05$, 0.01 and 0.001.

Results

The declining body weight gains of dams were statistically significant during Days 14-21 in the treated group, compared with the control group. The body weight suppression ratio in the treated group on Day 21 was 79% of the control group at the same time point. However, no dams showed any changes in clinical signs.

Table 1 shows the numbers and the weights of the live embryos/fetuses, the dead embryos/fetuses ratio, the placental weights at each sampling time point, and also the incidence of kinky tail on Day 21. The embryo weights in the treated group on Days 15 and 16 were statistically lower than that of the control group. In the treated group on Day 21, all fetuses showed small size and a reduction of body weight statistically with microphthalmia and microencephaly (Fig. 2). The incidence of kinky tail was 72.7%. The placental weights were statistically lower than those of the control group. Macroscopically, the edges of these placentas appeared white. No other external malformations were observed in any groups. The absolute and relative brain weight and the length ratio of cerebrum in the treated group were reduced significantly in comparison with the control group (Table 2). These brains were characterized by poor

development of the cerebrum.

Histological examination on gestation days 14.5, 15, and 16

Neuroepithelial cells, characterized by pyknosis or karyorrhexis, phagocytosis, and cell debris were seen in the telencephalon, diencephalon, mesencephalon, and metencephalon of the embryos on Days 14.5 and 15. Although cell death in the treated brain remained in the telencephalon, diencephalon and mesencephalon until Day 16, the degree of cell death in brain gradually decreased or disappeared following withdrawal. Table 3 shows the distribution of pyknosis or karyorrhexis in each location at each sampling time. Most of these pykonotic cells were stained by TUNEL method. On Day 14.5, they were observed mainly in the medial and dorsal layer of the neuroepithelium with a reduction of neuroepithelial cell density. In addition to these areas, they were also seen in the preplate on Day 15 (Fig. 3). On Day 16, they were located in the dorsal layer of the neuroepithelium and the intermediate zone in the telencephalon (Fig. 3). A marked reduction of thickness of the cortex, including the neuroepithelium, a slight stenosis of the cerebral ventricle and a decrease in cell density in the subventricular zone were observed in the telencephalon. The mitotic index in the neuroepithelium in the telencephalon on Days 14, 15 and 16 appeared to be significantly decreased in comparison with the control group (Fig. 4).

In the eye, pyknosis or karyorrhexis and phagocytosis were seen in the neural retina with a reduction of thickness and cell density in the treated

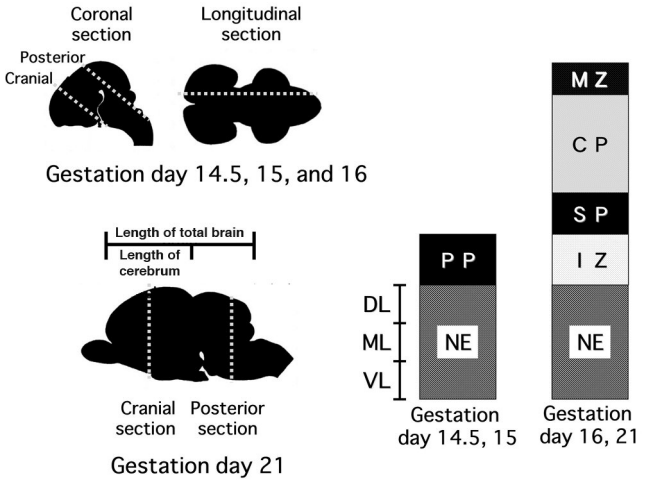

Fig. 1. Brain trimmed and measured sections (Left side) and nomenclature for layers of developing brain (Right side). NE: Neuroepithelium, VL: Ventricular layer (Subventricular layer), ML: Medial layer, DL: Dorsal layer, PP: Preplate, IZ: Intermediate zone (Intermediate cortical layer), SP: Subplate, CP: Cortical plate, MZ: Marginal zone (Cortical layer 1).

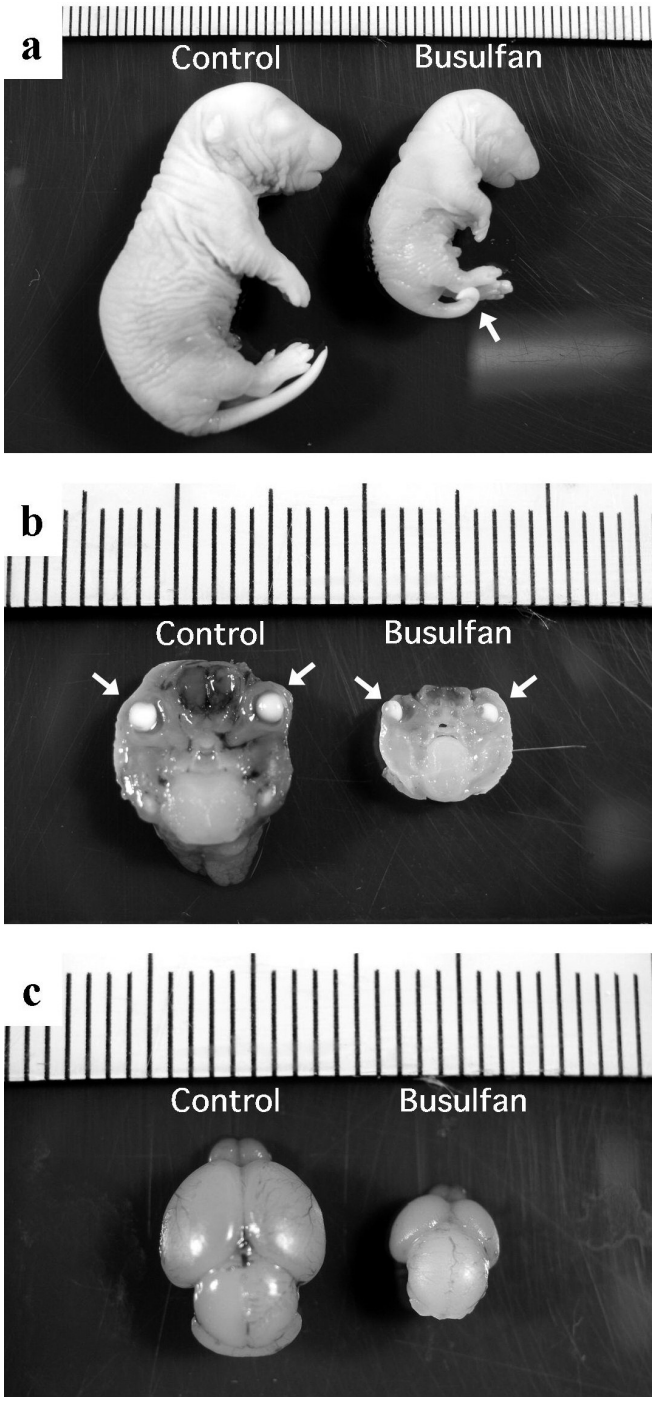

Fig. 2. Gross appearance of fetuses, fetal brains and coronal sections of eye on gestation day 21. **a.** Gross appearance of fetus of control (left) and busulfan (right). Body size is apparently smaller with kinky tail (arrow) in busulfan-treated rat. **b.** Coronal sections of eye (arrows) of control (left) and busulfan (right). Fetal eye of busulfan-treated rat reduces in size. **c.** Gross appearance of fetal brain of control (left) and busulfan (right). Fetal brain of busulfan-treated rat exhibits a reduction in size.

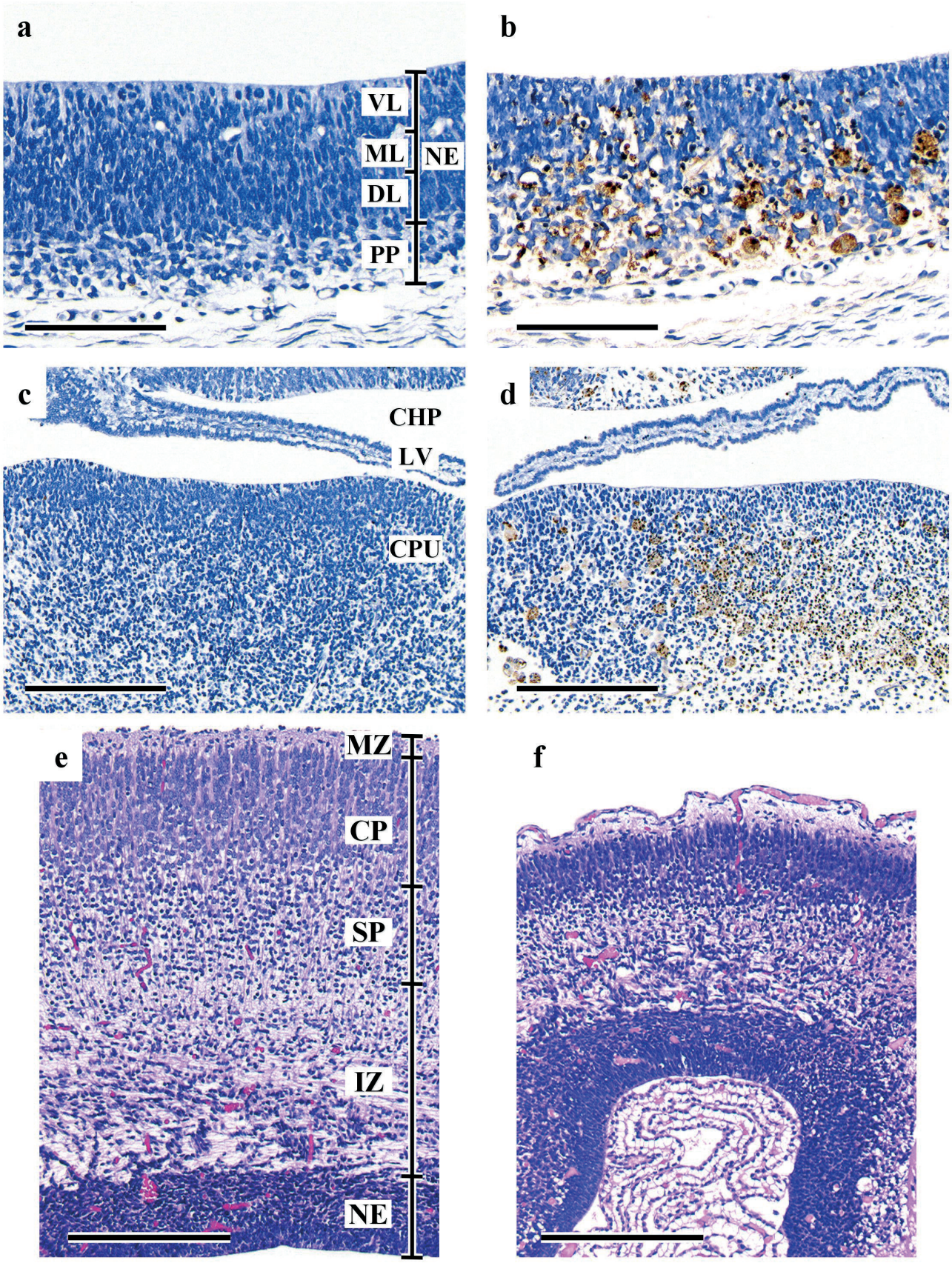
a
VL
ML
NE
DL
PP
b
c
CHP
LV
CPU
d
e
MZ
CP
SP
IZ
NE
f

group on Days 14.5, 15 and 16 (Fig. 5). Most of these cells were stained by TUNEL method as in the brain. In the lens, an increase in pyknosis or karyorrhexis in the lens epithelial cells and a depression of cell density in the nuclear bow were observed in comparison with the control group (Fig. 5). In addition to these lesions, cell

Table 1. Effect of busulfan on embruos/fetuses, placentas and kinky tail.

Gestation day	Group	Total No. of live embryos/fetuses	Dead embryo/ fetus ratio (%)[a]	Embryo/fetus weight (g)[a]	Placenta weight (g)[a]	Incidence of kinky tail (%)[a]
14.5	Control	49	4.2±2.4	0.177±0.007	0.144±0.009	NE
	Busulfan	48	5.6±1.9	0.158±0.003	0.153±0.015	NE
15	Control	49	6.3±6.3	0.291±0.009	0.245±0.018	NE
	Busulfan	48	2.3±2.3	0.244±0.007**	0.221±0.006	NE
16	Control	52	11.2±4.6	0.471±0.020	0.279±0.020	NE
	Busulfan	34	13.8±5.5	0.356±0.037***	0.294±0.037	NE
21	Control	50	0.0±0.0	4.806±0.075	0.456±0.016	0.0±0.0
	Busulfan	45	5.8±3.7	1.751±0.132***	0.260±0.017***	72.7±24.3

NE: Not examined; Mean±SE; [a]: Mean of individual litter values; **, ***: Significantly different from control at p<0.01, p<0.001, respectively (student *t*-test)

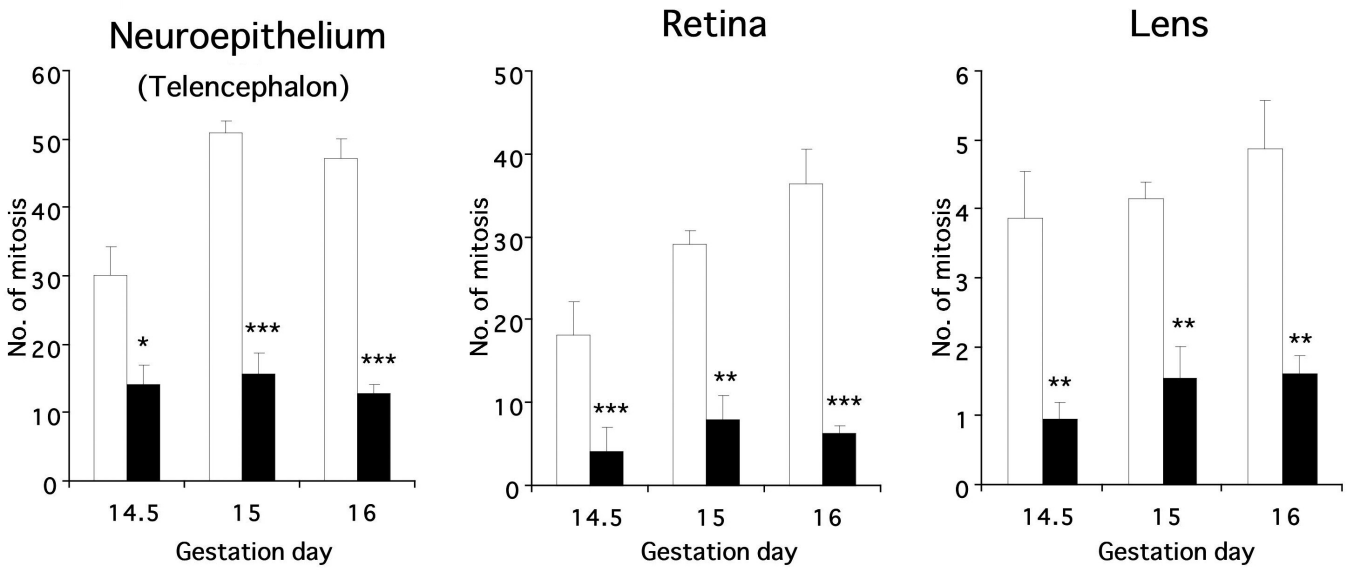

Fig. 4. Mitotic index in neuroepithelium in telencephalon, retina and lens on gestation days 14.5, 15 and 16. white bars: control, black bars: busulfan. Each value represents mean ± SE. *, **, ***: Significantly different from control at p<0.05, p<0.01, p<0.001 (Student *t*-test). The mitotic index of each tissue on Days 14, 15 and 16 appeared to be significantly decreased.

Fig. 3. Distribution of TUNEL-positive cells in neuroepithelium on gestation days 15 and 16, and morphological changes (HE stain) in cerebrum on gestation day 21. NE: Neuroepithelium, VL: Ventricular layer, ML: Medial layer, DL: Dorsal layer, PP: Preplate, IZ: Intermediate zone, SP: Subplate, CP: Cortical plate, MZ: Marginal zone, CHP: choroid plexus, CPU: caudate putamen neuroepithelium, LV: lateral ventricle. **a, b.** TUNEL stain of control **(a)** and busulfan **(b)**. Neuroepithelium in cortex in the cranial telencephalon on Day 15. TUNEL-positive cells are present in the medial and dorsal layers of the neuroepithelium and the prepalate with a reduction of neuroepithelial cell density in busulfan-treated rat. Bar: 100µm. **c, d.** TUNEL stain of control **(c)** and busulfan **(d)**. Caudate putamen neuroepithelium in the cranial telencephalon on Day 16. TUNEL-positive cells are present in the neuroepithelium with a reduction of cell density. Bar: 200µm. **e, f.** HE stain of control **(e)** and busulfan **(f)**. Cerebral cortex on Day 21. Cortex became markedly thinner with a reduction of the cortical plate, subplate and intermediate zone, and an increase in cell packing density. Dilatation of the cerebral ventricle was observed filled with the choroid plexus. Bar: 400µm.

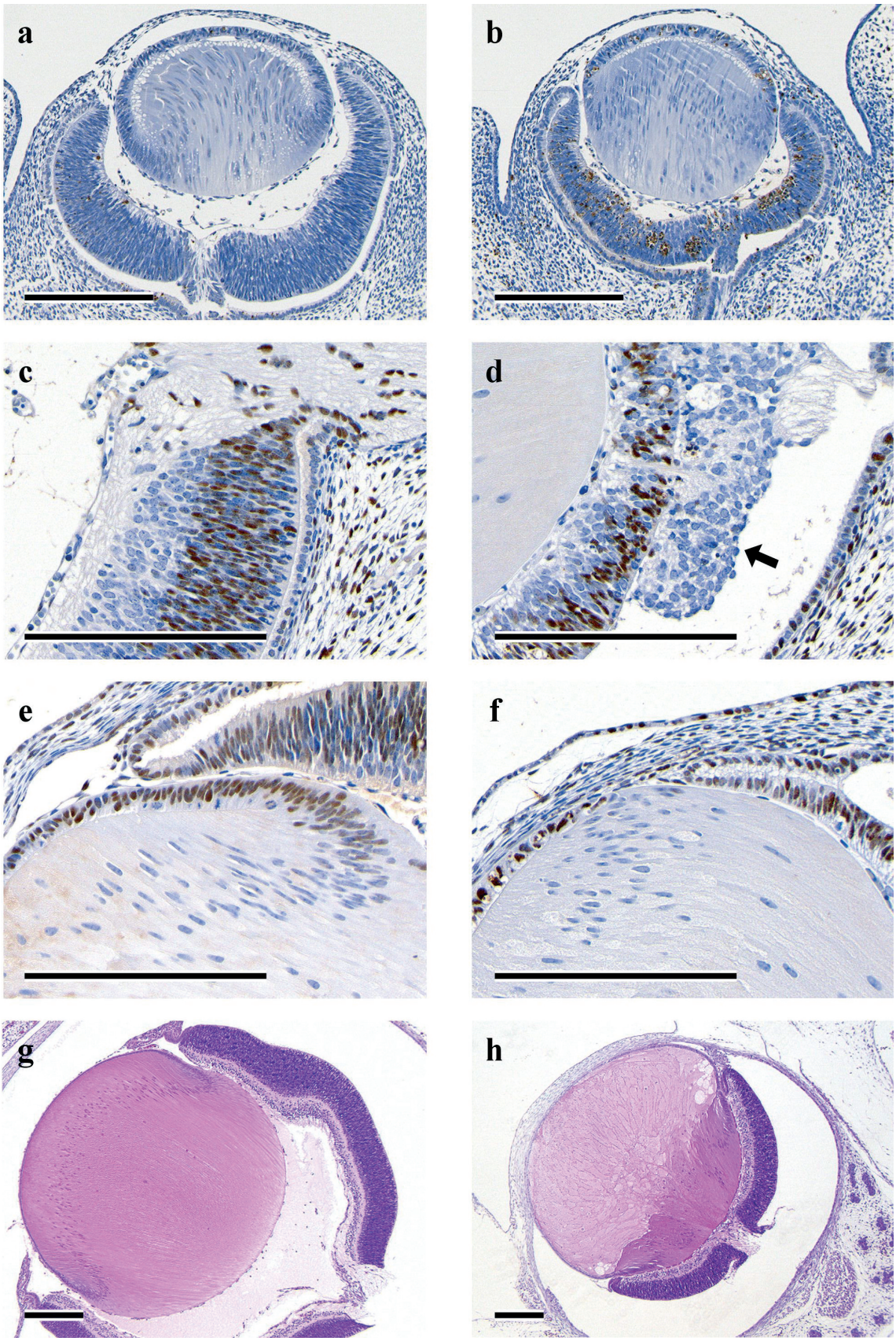

Fig. 5. Distribution of TUNEL-positive cells in retina on gestation day 14.5, distribution of PCNA-positive cells in retina and lens on gestation day 16 and morphological changes (HE stain) in eye on gestation day 21. **a, b.** TUNEL stain of control **(a)** and busulfan **(b)**. Eye on Day 14.5. TUNEL-positive cells are present in the neural retina with a width reduction in busulfan-treated rat. **c, d.** PCNA stain of control **(c)** and busulfan **(d)**. Center region of the retina on Day 16. A decrease in PCNA-positive nuclei is observed in the thinning neural retina in busulfan-treated rat. Cell mass (arrow) connected with the neural retina is located in the intra-retinal space. **e, f.** PCNA stain of control **(e)** and busulfan **(f)**. Equatorial zone of the lens on Day 16. A decrease in PCNA-positive nuclei and a reduction of cell density is observed in the nuclei bow and the equatorial zone of the lens in busulfan-treated rat. **g, h.** HE stain of control **(g)** and busulfan **(h).** Eye on Day 21. The retina exhibits hypoplasia with a reduction of thickness of the outer nuclear layer and outerplexiform layer. Swollen, fragmentary and vacuolar lens fibers in the anterior region and poor development of the posterior region in busulfan-treated rats. Bar: 200 μm

death was also slightly noted in the optic stalk in some of the embryos in the treated group on Days 14.5 and 15. Irregular cell masses were observed in the intra-retinal space attached to the retina on Day 16. These masses seemed to consist of the retinal cells. PCNA positive cells were decreased at the equatorial zone and the neural retina in the treated group as compared with the control group (Fig. 5). A statistically significant decrease in mitotic index was detected in the lens and neural retina in the treated group on Days 14.5, 15 and 16 (Fig. 4). There were no apparent morphological changes in the control group.

Histological examination on gestation day 21

In comparison with the control group, the cerebral cortex in the treated group became markedly thinner with a reduction of the cortical plate, subplate and intermediate zone, and an increase in cell packing density (Fig. 3). Dilatation of the cerebral ventricle was observed filled with the choroid plexus. In the eye, the thickness of the outer nuclear layer and outerplexiform layer of the retina were reduced as compared with the control group (Fig. 5). The lens fibers showed swollen, fragmentary and vacuolar formation in the cranial portion, and the development of the secondary lens fibers was poor in the posterior portion of the lens, accompanied with small sized lens in the treated fetuses. Nuclei remained in some lens fibers.

Electron microscopic examination on gestation day 14.5

Pyknotic cells in the medial and dorsal layer of neuroepithelium with appearance of cell death characterized by shrinkage of the cell body with high

Table 2. Fetal brain weight on gestation day 21.

Group	Absolute brain weight (mg)	Relative brain weight (% B.W.)	Length ratio of cerebrum (%) (cerebrum/total brain)
Control	223.4±5.4	4.62±0.07	66.63±0.75
Busulfan	74.0±5.6***	3.97±0.21*	52.75±0.95***

Mean±SE; a: Mean of individual litter values; *, ***: Significantly different from control at p<0.05, p<0.001, respectively (student *t*-test)

Table 3. Distribution of cell death in developing brain and eye

Regions	Gestation day		
	Day 14.5	Day 15	Day 16
Brain			
Telencephalon	++	++	+
Diencephalon	++	+	+
Mesencephalon	+	+	±
Metencephalon	+	±	-
Eye			
Retina	+	+	+
Lens	±	±	±

Codes: -: almost absent, ±: slight, +: mild, ++: moderate, +++: severe

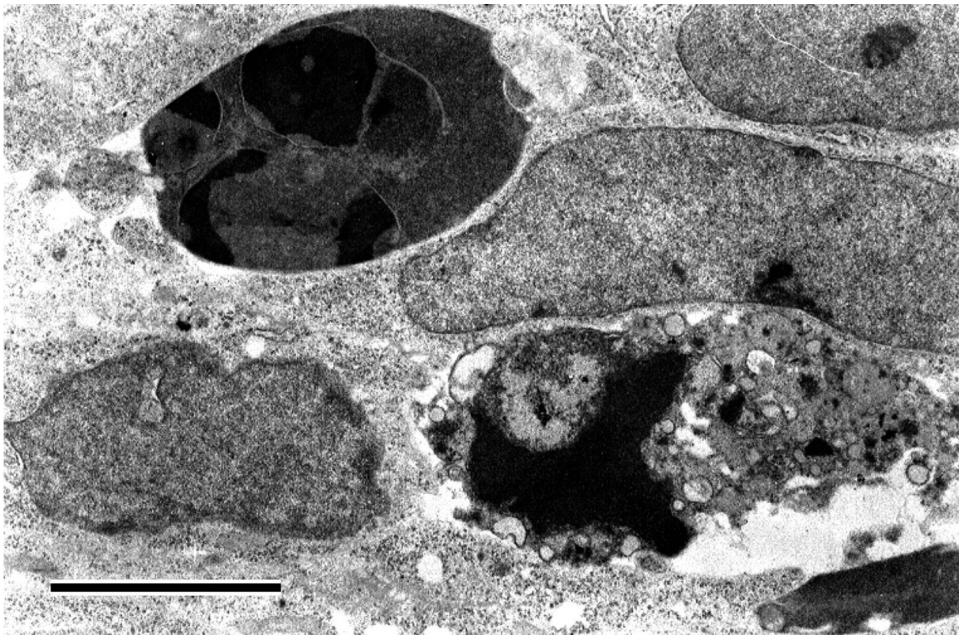

Fig. 6. Electron micrograph of pyknotic cell in neuroepithelium in busulfan treated embryo on gestation day 14.5. Nuclear chromatin of the cell is fragmented in to high electron density with the condensation and shrinkage of the cytoplasm, termed “apoptotic bodies”. Macrophage engulfs fragmented apoptotic bodies. Surrounding neuroepithelial cells are intact. Bar: 5 μm

electron density of fragmented nuclear chromatin, termed "apoptotic bodies", were seen in the telencephalon of busulfan-treated group. Surrounding neuroepithelial cells were intact (Fig. 6).

Discussion

The results of our experiments indicated that microencephaly and microphthalmia were found in rat fetuses following the maternal intraperitoneal administration of busulfan at 10 mg/kg/day during Days 12-14. Histopathologically, busulfan induced cell death and mitotic inhibition of the neuroepithelium, neural retina and lens in the embryos. It was confirmed that these cell deaths were considered to be apoptosis, as demonstrated by the TUNEL method, which detects fragmented DNA *in situ*, and in addition, electron microscopic observation of condensed nuclear fragments within macrophages.

Induced-microencephaly has been reported in fetal rats following exposure to γ- and X-radiation (Hoshino and Kameyama, 1988), administration of ethanol (Miller, 1986), 1-ß-D-arabinofuranosylcytosine (Ara-C) (Yamauchi et al., 2003), 5-azacytidine (Lu et al., 1998; Ueno et al., 2002a,b), ethylnitrosourea (ENU) (Katayama et al., 2000a,b), indole acetic acid (Furukawa et al., 2004), and methylazoxymethanol (Cattabeni and Di Luca, 1997), etc. Some substances cause apoptosis in the neuroepithelial cells, and in turn induce excessive neuron death in developing cerebral cortex (Brill et al., 1999). In our study, busulfan-induced apoptotic cells were increased mainly in the medial and dorsal layer of the neuroepithelium, where G1, G2 and S phase cells located, on Days 13.5 and 14. Furthermore, there was a reduction of mitotic activity in the neuroepithelium. Busulfan produces crosslinks in DNA through a four-carbon bridge by displacement of one and then the other methylsufonate and the cells are most sensitive in the late G1-phase. They pass normally through S-phase but are unable to undergo normal mitosis (Grimes, 1964). In addition, a progression through the cell cycle is blocked in the G2-phase, as in other alkylating agents (Buggia et al., 1994; Hung et al., 1996). Therefore, we suspected that busulfan might induce cell cycle arrest in G1/G2-phase and DNA damage, and lead to apoptosis and mitotic inhibition in the neuroepithelium. The decrease in newborn neurons could bring about a lack of cell populations required for later normal histogenesis and organogenesis, resulting in microencephaly. Further detailed investigations of the activated genes in relationship with busulfan-induced apoptosis are necessary to clarify the mechanisms of neuronal apoptosis.

Induced microphthalmia has been reported in fetal rats following exposure to X-radiation (Kuno et al., 1992), cyclophosphamide (Singh and Sanyal, 1976), trypan blue (Schmidt et al., 1983), 6-aminonicotinamide (Szabo, 1989), etc. and the lack of panthothenic acid or zinc (Szabo, 1989). As mentioned in the introduction, some mechanisms of microphthalmia have been reported. Primary microphthalmia or anophthalmia is due to failure of formation of the optic anlage from the forebrain during differentiation of the optic plate. This type is usually not accompanied by neural anomalies. Secondary type due to complete suppression or abnormal development of the entire region of the forebrain is associated with brain malformation. The third type results from the breakdown and degeneration of the optic vesicle after its formation (Szabo, 1989). Trypan blue and 6-aminonicotinamide-induced microphthalmia is attributed to failure of the optic vesicle development. Cyclophosphamide induces failure of the retinal development. Furthermore, spontaneous microphthalmia of the Msx2 transgenic mice (Wu et al., 2003), and Nuc1 mutation rats (Sinha et al., 2004) are caused by an inhibition of lens fiber cell differentiation and an increase in retinal cell death, and a disruption of lens and a thickening of the retina attributed to prevent apoptosis, respectively. In our study, we observed a marked increase in apoptosis and a decrease in mitotic activity in the neural retina during the optic organogenesis and resultant hypoplasia of the retina, which might have been caused by the same mechanisms as the neuroepithelial lesions in the brain as described above. On the other hand, the lens on Day 21 exhibited lens fiber degeneration and poor development of the secondary lens fibers. The lesions of lens fiber degeneration were previously described in humans receiving busulfan treatment for leukemia (Hamming, 1976; Kaida, 1999). Cataract was seen in rats exposed to ten times the therapeutic level in prolonged administration studies (von Sallmann, 1957). The opacification appears to result from a profound inhibition of cell proliferation in the lens epithelium which affects the cell cycle (Grimes, 1964). The fetal lens lesions seen in our study could have resulted from mitotic inhibition in the equatorial zone, normally the area of maximum mitotic activity and apoptosis in the lens epithelial cells during their organogenesis. Therefore, we suggest that the busulfan-induced microphthalmia might be attributed to inhibition of the developing retina and the lens by excessive cell death and mitotic inhibition after the optic vesicle formation, and might not be associated with suppression of the forebrain growth or microencephaly.

In conclusion, busulfan induced apoptosis and mitotic inhibition in the neuroepithelium, retina and lens in the embryos. The anti-proliferative effects of busulfan could have inhibited the development of the cerebral cortex and eye, and induced microencephaly and microphthalmia, featuring hypoplasia of cerebrum and hypoplasia of retina and lens with cataract, respectively.

Acknowledgements. The authors would like to thank Mr. Kiyoshi Kobayashi, Ms. Kaori Maejima, Ms. Hideko Ishibashi, Mr. Atsushi Funakoshi, Mr. Yoshinori Tanaka, Ms. Mayumi Seta, Ms. Hiromi Asako, and Mr. Shigeru Iimura for their excellent technical assistance.

References

Bayer S.A. and Altman J. (2004). Development of the telencephalon: Neural stem cells, neurogenesis, and neuronal migration. In: The rat Nervous system. 3rd ed. Paxions G. (ed.) Elsevier Academic Press. San Diego. pp 27-73.

Bishop J.B. and Wassom J.S. (1986). Toxicological review of busulfan (Myleran). Mutat. Res. 168, 15-45.

Brill A., Torchinsky A., Carp H. and Toder V. (1999). The role of apoptosis in normal and abnormal embryonic development. J. Assist. Reprod. Genet. 16, 512-519.

Buggia I., Locatelli F., Regazzi M.B. and Zecca M. (1994). Busulfan. Ann. Pharmacother. 28, 1055-1062.

Cattabeni F. and Di Luca M. (1997). Developmental models of brain dysfunctions induced by targeted cellular ablations with methylazoxymethanol. Physiol. Rev. 77, 199-215.

DeSesso J.M. (2005). Comparative features of vertebrate embryology. In: Developmental and reproductive toxicology. A practical approach. 2nd ed. Hood R.D. (ed). Taylor & Francis. Boca Raton. pp 147-197.

Furukawa S., Abe M., Usuda K. and Ogawa I. (2004). Indole-3-acetic acid induces microencephaly in rat fetuses. Toxicol. Pathol. 32, 659-667.

Gressens P. (2000). Mechanisms and disturbances of neuronal migration. Pediatr. Res. 48, 725-730.

Grimes P. (1964). Influence of myleran on cell proliferation in the lens epithelium. Invest. Ophthalmol. 47, 566-576.

Hamming N.A. (1976). Histopathology and ultrastructure of busulfan-induced cataract. Albrecht von Graefes Arch. Klin. Exp. Ophthalmol. 200, 139-147.

Hirshfield A.N. (1994). Relationship between the supply of primordial follicles and the onset of follicular growth in rats. Biol. Reprod. 50, 421-428.

Hoshino K. and Kameyama Y. (1988). Developmental-stage-dependent radiosensitivity of neural cells in the ventricular zone of telencephalon in mouse and rat fetuses. Teratology 37, 257-262.

Hung D.T., Jamison T.F. and Schreiber S.L. (1996). Understanding and controlling the cell cycle with natural products. Chem. Biol. 3,623–639.

Kaida T. (1999). Cataract induced by short-term administration of large doses of busulfan: A case report. Ophthalmologica 213, 397-399.

Kasuga F. and Takahashi M. (1986). The endocrine function of rat gonads with reduced number of germ cells following busulphan treatment. Endocrinol. Jpn. 33, 105-115.

Katayama K., Ishigami N., Suzuki M., Ohtsuka R., Kiatipattanasakul W., Nakayama H. and Doi K. (2000a). Teratologic studies on rat perinates and offspring from dams treated with ethylnitrosourea (ENU). Exp. Anim. 49, 181-187.

Katayama K., Ishigami M., Uetsuka K., Nakayama H. and Doi, K. (2000b). Ethylnitrosourea (ENU)-induced apoptosis in the rat fetal tissues. Histol. Histopathol. 15, 707-711.

Kuno H., Inagaki S., Ban Y., Konishi R., Tanaka K., Fujii T. and Usui T. (1992). Usefulness of ophthalmic examination in postnatal observation in teratology studies. Jikken Dobutsu 41, 363-367.

Lu D.P., Nakayama H., Shinozuka J., Uetsuka K., Taki R. and Doi K. (1998). 5-azacytidine-induced apoptosis in the central nervous system of developing rat fetuses. J. Toxicol. Pathol. 11, 133-136.

Miller M.W. (1986). Effects of alcohol on the generation and migration of cerebral cortical neurons. Science 233, 1308-1311.

Nagai H. (1972). Effects of transplacentally injected alkylating agents upon development of embryos. Appearance of intrauterine death and mesodermal malformation. Bull. Tokyo Dent. Coll. 13, 103-119.

O'Leary D.D.M. and Koester S.E. (1993). Development of projection neuron types, axon pathways, and patterned connections of the mammalian cortex. Neuron 10, 991-1006.

Rice D. and Barone S.J. (2000). Critical periods of vulnerability for the developing nervous system: Evidence from humans and animal models. Environ. Health Perspect. 108, 511-533.

von Sallmann L. (1957). The lens epithelium in the pathogenesis of cataract. Trans. Am. Acad. Ophthalmol. Otolaryngol. 61, 7-19.

Schmidt K.L., Milner K., Hilburn P.J. and Schmidt W.A. (1983). Ultrastructure of trypan blue induced ocular defects: I. Retina and lens. Teratology 28, 131-144.

Singh S. and Sanyal A.K. (1976). Eye anomalies induced by cyclophosphamide in rat fetuses. Acta Anat. (Basel). 94, 490-496.

Sinha D., Hose S., Zhang C., Neal R., Ghosh M., O'Brien T.P., Sundin O., Goldberg M.F., Robison W.G.J., Russell P., Lo W.K. and Zigler S.J. (2005). A spontaneous mutation affects programmed cell death during development of the rat eye. Exp. Eye Res. 80, 323-335.

Szabo K.T. (1989). Sensory system. In: Congenital malformations in laboratory and farm animals. 1st ed. Szabo K.T. (ed). Academic Press. San Diego. pp 245-268.

Ueno M., Katayama K., Nakayama H. and Doi K. (2002a). Mechanisms of 5-azacytidine (5Az-C)-induced toxicity in the rat brain. Int. J. Exp. Path. 83, 139-150.

Ueno M., Katayama K., Yasoshima A., Nakayama H. and Doi K. (2002b). 5-Azacytidine (5AzC)-induced histopathological changes in the central nervous system of rat fetuses. Exp. Toxicol. Pathol. 54, 91-96.

Yamauchi H., Katayama K., Yasohima A., Uetsuka K., Nakayama H. and Doi K. (2003). 1-ß-D-arabinofuranosylcytosine (Ara-C)-induced apoptosis in the rat fetal tissues and placenta. J. Toxicol. Pathol. 16, 223-229.

Wu L.Y., Li M., Hinton D.R., Guo L., Jiang S., Wang J.T., Zeng A., Xie J.B., Snead M., Shuler C., Maxson R.E.Jr. and Liu Y.H. (2003). Microphthalmia resulting from MSX2-induced apoptosis in the optic vesicle. Invest. Ophthalmol. Vis. Sci. 44, 2404-2412.

Accepted October 20, 2006